Available online at www.sciencedirect.com
ScienceDirect
International Journal of Thermal Sciences 48 (2009) 1026–1035
International Journal of Thermal Sciences
www.elsevier.com/locate/ijts

A comparative study of viscous dissipation effect on entropy generation in single-phase liquid flow in microchannels

Yew-Mun Hung *

Faculty of Engineering and Technology, Multimedia University, 75450 Melaka, Malaysia

Received 8 December 2007; received in revised form 3 July 2008; accepted 30 July 2008

Available online 22 August 2008

Abstract

The influence of viscous dissipation on entropy generation in fully developed forced convection for single-phase liquid flow in a circular microchannel under imposed uniform wall heat flux has been studied. In the first-law analysis, closed form solutions of the radial temperature profiles for the models with and without viscous dissipation term in the energy equation are obtained. In the second-law analysis, for different Brinkman number and dimensionless heat flux, the variations of dimensionless entropy generation and Bejan number as a function of the radial distance are investigated. The two models are compared by analyzing their relative deviations in dimensionless entropy generation and Bejan number. Comparisons are also performed for average dimensionless entropy generation and average Bejan number. Contribution of heat transfer irreversibility and fluid friction irreversibility to the deviations is analyzed and discussed. It is found that, under certain conditions, the effect of viscous dissipation on entropy generation in microchannel is significant and should not be neglected.

Keywords: Viscous dissipation; Entropy generation; Irreversibility; Brinkman number; Bejan number; Microchannel

1. Introduction

Fluid transport in microchannels plays a vital role in a wide variety of contemporary engineering applications, involving micro-scale devices such as micropumps, microvalves and microsensors. Particularly, the application of microchannels in electronic cooling is becoming tremendously important due to the increasingly high-flux heat generation from high-speed microprocessors. The extensive use of microchannels, therefore, has promoted abundant studies on their fluid flow and heat transfer characteristics. In addition to the analysis based on the basic conservation laws, the second-law analysis is essential in understanding the entropy generation, which is attributed to the thermodynamic irreversibility. This kind of thermodynamic analysis is useful for studying the optimum operating conditions, which help in designing a system with less entropy and destruction of available work (exergy), in accordance to the Gouy–Stodola theorem stating that the lost available work is directly proportional to the entropy generation. Bejan [1] referred this method of engineering research as Entropy Generation Minimization (EGM) and discussed its derivations and applications in a vast coverage of applied thermal engineering. The importance of understanding the intricacies of entropy generation in heat transfer devices has attracted much attention henceforth. From the point of view of an engineering design consideration, the performance evaluation criteria, such as heat transfer surface performance based on the second law of thermodynamics [2] are intimately related to entropy generation assessments.

Viscous dissipation manifests itself as an appreciable rise in fluid temperature due to the conversion of kinetic motion of the fluid to thermal energy, and features as a source term in the fluid flow. This effect is of particular significance in fluid flow and heat transfer in microchannel whose length-to-diameter ratio is considerably large. The importance of viscous dissipation can be quantified by a dimensionless number, i.e. Brinkman number, which is defined as the ratio of the heat generation due to viscous forces to the heat transferred from the wall to the fluid. Tso and Mahulikar [3] proposed Brinkman number as a parameter for correlating the convective heat transfer parame-

* Tel.: +606 252 3791; fax: +606 231 6552.
E-mail address: hungyewmun@gmail.com.

1290-0729/$ – see front matter
doi:10.1016/j.ijthermalsci.2008.07.011

Nomenclature

A_c	cross-sectional area	m^2
Be	Bejan number	
$\overline{Be}$	average Bejan number	
Br'	Brinkman number based on uniform heat flux condition	
c_p	specific heat	$J\,kg^{-1}\,K^{-1}$
D_H	hydraulic diameter of microchannel	m
k	thermal conductivity	$W\,m^{-1}\,K^{-1}$
m	pertinent parameters, as defined in Eq. (29)	
N_S	dimensionless entropy generation	
$\bar{N}_S$	average dimensionless entropy generation	
Pe	Péclet number	
q_w	uniform wall heat flux	$W\,m^{-2}$
r	radial coordinate	m
r_0	internal radius of microchannel	m
R	dimensionless radial coordinate	
$\dot{S}'''_{gen}$	volumetric rate of entropy generation	$W\,m^{-3}\,K^{-1}$
T	temperature	K
$\bar{T}$	bulk mean temperature	K
u	fluid velocity	$m\,s^{-1}$
$\bar{u}$	mean velocity of fluid	$m\,s^{-1}$
$\hat{u}$	dimensionless fluid velocity	
x	longitudinal coordinate	m

Greek symbols

δ	relative deviation of pertinent parameters, as defined in Eq. (29)	%
θ	dimensionless temperature	
μ	fluid viscosity	$N\,s\,m^{-2}$
ρ	fluid density	$kg\,m^{-3}$
ϕ	irreversibility distribution ratio	
Φ	viscous dissipation function	s^{-2}
ψ	dimensionless heat flux	

Subscripts

FF	fluid friction
HT	heat transfer
w	value at wall
1	model with viscous dissipation
2	model without viscous dissipation

ters in microchannels. Brinkman number was used to explain the unusual heat transfer behaviour in microchannels, which significantly differs from that in the conventionally-sized channels. Later, they [4] performed experiments to verify the role of Brinkman number in the laminar regime in microchannels. Judy et al. [5], according to their experimental data, reported that viscous dissipation induces significant effect of increasing the fluid temperature along the microchannel length for decreasing diameter and increasing fluid velocity. Koo and Kleinstreuer [6], employing scale analyses and numerical solutions, investigated the viscous dissipation effects on the evolution of temperature distributions for different working fluids and channel geometries, and concluded that the impact of viscous dissipation on microchannel flow is significant and should be taken into consideration for all experimental and computational analyses. Morini [7] used a mathematical model to assess the significance of viscous dissipation in microchannel flows and declared that the viscous dissipation effect is important for liquid flows when the hydraulic diameter is less than 100 μm. Hetsroni et al. [8] discussed the effect of viscous dissipation which may lead to drastic change of flow and temperature fields in microchannels under certain conditions. It is validated from previous studies that the effect of viscous dissipation is significant in the first-law analysis of fluid transport in microchannels, in which the main concern is the flow and temperature distributions. Judging from this, it is instructive to conceive that in the second-law analysis, the viscous dissipation effect should also be taken into consideration in the derivation of the entropy generation rate in microchannels, which is strongly dependent on the flow and temperature fields of the fluid.

Many of the existing analytical studies on entropy generation in macro-scale channel and duct flow passages neglected the effect of viscous dissipation in the energy equation, such as those in [9–17]. On the contrary, there exist a very small number of studies that dealt with entropy generation related problems in micro-scale channels. Richardson et al. [18] explored the existence of irreversibility extrema in the laminar flow region inside straight microchannels with irregular cross sections. They solved the momentum and energy equations numerically. However, the viscous dissipation term was not considered in the energy equation. Recently, Erbay et al. [19] investigated the entropy generation in parallel plate microchannels induced by the transient laminar forced convection in the combined entrance region numerically. On the other hand, Abbassi [20] analyzed analytically the entropy generation in a uniformly heated rectangular microchannel heat sink by applying a porous medium model based on extended Darcy equation for fluid flow and two-equation model for heat transfer. However, the viscous dissipation term was neglected in the energy equation for the fluid phase in these studies. The rationale of neglecting viscous dissipation effect in the energy equation (first-law analysis) is questionable as the fluid friction irreversibility due to frictional heating of viscous dissipation plays a vital role in the second-law analysis. In addition, it is indisputable that the entropy generation is strongly dependent on the temperature field of the fluid, which is intimately related to the irreversible energy conversion from viscous dissipation in the fluid. In view of this, it is well worth investigating the effect of viscous dissipation in the energy equation on the entropy generation derived from the second-law analysis in microchannels.

The primary concern of the present study is to compare the characteristics of the entropy generation in single-phase liquid flow in a circular microchannel between the models with and without viscous dissipation term in the energy equation. Em-

ploying the first principles to the hydrodynamically and thermally fully developed laminar flow, closed form solutions for the velocity and temperature distributions in the radial direction are obtained and then utilized in the computation of the local and average dimensionless entropy generation and Bejan number. Their characteristics and deviations from those without considering viscous dissipation are analyzed and discussed.

2. Mathematical formulation

2.1. First-law analysis

In dealing with single-phase liquid flows in microchannels, the flowing fluids are treated as continuous media and the continuum approximation employed in the conventional macro-scale flow system is applicable. Gad-el-Hak [21] pointed out that the traditional results obtained for macro-scale flow are applicable in channels larger than 1 μm. Following this, for a circular microchannel with internal radius r_0, under steady-state and fully developed conditions, the velocity profile of laminar flow for incompressible Newtonian fluid passing through the microchannel is given by the Hagen–Poiseuille expression as

$$u = 2\bar{u}\left[1 - \left(\frac{r}{r_0}\right)^2\right] \tag{1}$$

where $\bar{u}$ is the mean velocity over the cross section area of the microchannel. For constant fluid properties, the energy equation is expressed as [22]

$$\rho c_p u \frac{\partial T}{\partial x} = \frac{k}{r}\frac{\partial}{\partial r}\left(r\frac{\partial T}{\partial r}\right) + \mu\left(\frac{\partial u}{\partial r}\right)^2 \tag{2}$$

where T is the temperature of the working fluid, c_p, k and μ are the specific heat, thermal conductivity and viscosity of the fluid, respectively. According to Wang and Peng [23], to simulate the heat generated by electronic components, the applied heat flux from the wall of the microchannel is rationally assumed to be uniformly distributed. Following this, under a fully developed thermal condition with uniformly heated boundary wall, the longitudinal conduction term is absent in the energy equation since its contribution to the net energy transfer is negligible [22,24]. Taking into account the frictional heating due to viscous dissipation, this effect is incorporated as the second term on the right-hand side in Eq. (2). The thermal boundary condition at the wall of the microchannel is expressed as

$$k\left.\frac{\partial T}{\partial r}\right|_{r=r_0} = q_w \tag{3a}$$

where q_w is the uniform heat flux applied at the wall. Another condition is the symmetric condition at the centre, which is written as

$$\left.\frac{\partial T}{\partial r}\right|_{r=0} = 0 \tag{3b}$$

The bulk mean temperature $\bar{T}$ is defined as

$$\bar{T} = \frac{2}{r_0^2\bar{u}}\int_0^{r_0} uTr\,dr \tag{4}$$

For uniformly heated wall condition and thermally fully developed flow, the temperature gradient along the axial direction is defined classically as

$$\frac{\partial T}{\partial x} = \frac{d\bar{T}}{dx} \tag{5}$$

which is independent of the radial direction. Integrating Eq. (2) over the cross section of the microchannel gives

$$\rho c_p \frac{\partial}{\partial x}\int_0^{r_0} uTr\,dr = kr\left.\frac{\partial T}{\partial r}\right|_0^{r_0} + \mu\int_0^{r_0}\left(\frac{\partial u}{\partial r}\right)^2 r\,dr \tag{6}$$

By utilizing Eqs. (1), (3), (4) and (5), Eq. (6) can be simplified as

$$\rho c_p \bar{u}\frac{d\bar{T}}{dx} = \frac{2}{r_0^2}(q_w r_0 + 4\mu\bar{u}^2) \tag{7}$$

which conforms to the energy balance over the cross section of the microchannel. In the case of thermally fully developed condition with uniform wall heat flux, from Eq. (7), it is observed that the axial temperature gradient is reduced to a constant. By introducing the following dimensionless variables

$$R = \frac{r}{r_0}, \qquad \hat{u} = \frac{u}{\bar{u}}, \qquad \theta = \frac{k(T - T_w)}{q_w D_H} \tag{8}$$

where D_H is the hydraulic diameter of microchannel and T_w denotes the wall temperature, and utilizing the energy balance relation in Eq. (7), Eq. (2) is nondimensionalized as

$$\frac{1}{R}\frac{d}{dR}\left(R\frac{d\theta}{dR}\right) = (1 + 8Br')\hat{u} - Br'\left(\frac{d\hat{u}}{dR}\right)^2 \tag{9}$$

where the term on the left-hand side corresponds to radial conduction while the first term and second term on the right-hand side are related to convection and viscous dissipation, respectively. $Br'$is the modified Brinkman number based on the uniform heat flux condition [24], a measure of the importance of the viscous dissipation term, defined as

$$Br' = \frac{\mu\bar{u}^2}{q_w D_H} \tag{10}$$

The dimensionless boundary conditions required for solving Eq. (9) are

$$\theta(1) = 0 \tag{11a}$$

$$\frac{d\theta(0)}{dR} = 0 \tag{11b}$$

Substituting the dimensionless velocity profile and its gradient into Eq. (9) and solving it yields the closed form dimensionless temperature profile as

$$\theta_1(R) = -\frac{1}{8}(1 + 16Br')R^4 + \frac{1}{2}(1 + 8Br')R^2 - \frac{3}{8}\left(1 + \frac{16}{3}Br'\right) \tag{12}$$

For the case when the viscous dissipation term is neglected in the energy equation, i.e. $Br' = 0$, the dimensionless temperature profile becomes

$$\theta_2(R) = -\frac{1}{8}R^4 + \frac{1}{2}R^2 - \frac{3}{8} \tag{13}$$

Hereafter, for the purpose of comparison of results, the model with viscous dissipation term incorporated in the energy equation is denoted as Model 1 (with subscript 1) and that without viscous dissipation term in the energy equation as Model 2 (with subscript 2).

2.2. Second-law analysis

Entropy is generated due to the presence of irreversibility, and entropy generation is adopted as a quantitative measure of the irreversibility associated with a process. The volumetric rate of entropy generation which arises due to the heat transfer and fluid friction losses, is expressed as [1]

$$\dot{S}'''_{\text{gen}} = \dot{S}'''_{\text{gen,HT}} + \dot{S}'''_{\text{gen,FF}} = \frac{k}{T^2}(\nabla T)^2 + \frac{\mu}{T}\Phi \tag{14}$$

where Φ is the viscous dissipation function. The first term on the right-hand side of Eq. (14) is attributable to the heat transfer in the direction of finite temperature gradients while the second term on the right-hand side is due to the viscous effects of fluid friction. In the present study, for fully developed forced convection in a circular microchannel, the volumetric rate of entropy generation reduces to

$$\dot{S}'''_{\text{gen}} = \frac{k}{T^2}\left[\left(\frac{\partial T}{\partial x}\right)^2 + \left(\frac{\partial T}{\partial r}\right)^2\right] + \frac{\mu}{T}\left(\frac{\partial u}{\partial r}\right)^2 \tag{15}$$

Following this, the dimensionless entropy generation (for Model 1) is derived as

$$\begin{aligned} N_{\text{S1}} &= \frac{\dot{S}'''_{\text{gen}} r_0^2}{k} = \left(\frac{\psi}{1+\psi\theta_1}\right)^2\left[\left(\frac{d\theta_1}{dR}\right)^2 + \frac{4(1+8Br')^2}{Pe^2}\right] \\ &\quad + Br'\left(\frac{\psi}{1+\psi\theta_1}\right)\left(\frac{d\hat{u}}{dR}\right)^2 \\ &= 16\big\{(16Br'+1)(8Br'+1)R^6 - 4(8Br'+1)^2R^4 \\ &\quad + 4\big[32Br' + 2Br'(8/\psi+5) + 1\big]R^2 \\ &\quad + 16(8Br'+1)^2/Pe^2\big\} \\ &\quad \big/\big[(16Br'+1)R^4 - 4(8Br'+1)R^2 \\ &\quad + 16Br' - 8/\psi + 3\big]^2 \end{aligned} \tag{16}$$

where

$$\psi = \frac{q_{\text{w}} D_{\text{H}}}{k T_{\text{w}}} \tag{17}$$

is denoted as dimensionless heat flux, and

$$Pe = \frac{\rho c_{\text{p}} \bar{u} D_{\text{H}}}{k} \tag{18}$$

is Péclet number, indicating the relative importance between convection and conduction. The dimensionless entropy generation due to conductive heat transfer in radial and axial directions is correspondingly expressed as

$$\begin{aligned} N_{\text{HT1}} &= \left(\frac{\psi}{1+\psi\theta_1}\right)^2\left[\left(\frac{d\theta_1}{dR}\right)^2 + \frac{4(1+8Br')^2}{Pe^2}\right] \\ &= 16\big[(16Br'+1)^2R^6 - 4(16Br'+1)(8Br'+1)R^4 \\ &\quad + 4(8Br'+1)^2R^2 + 16(8Br'+1)^2/Pe^2\big] \\ &\quad \big/\big[(16Br'+1)R^4 - 4(8Br'+1)R^2 \\ &\quad + 16Br' - 8/\psi + 3\big]^2 \end{aligned} \tag{19}$$

and the dimensionless form of entropy generation contributed by fluid friction is written as

$$\begin{aligned} N_{\text{FF1}} &= Br'\left(\frac{\psi}{1+\psi\theta_1}\right)\left(\frac{d\hat{u}}{dR}\right)^2 \\ &= -128Br'R^2\big/\big[(16Br'+1)R^4 - 4(8Br'+1)R^2 \\ &\quad + 16Br' - 8/\psi + 3\big]. \end{aligned} \tag{20}$$

The relative significant contribution of these two terms is evaluated by the irreversibility distribution ratio ϕ, which is expressed as [1]

$$\phi = \frac{\dot{S}'''_{\text{FF}}}{\dot{S}'''_{\text{HT}}} = \frac{N_{\text{FF}}}{N_{\text{HT}}} \tag{21}$$

An alternative irreversibility distribution parameter, Bejan number Be, defined as the ratio of entropy generated due to heat transfer to total entropy generation, is expressed as

$$\begin{aligned} Be_1 &= \frac{N_{\text{HT}}}{N_{\text{S}}} \\ &= \frac{(\frac{d\theta_1}{dR})^2 + [2(1+8Br')/Pe]^2}{(\frac{d\theta_1}{dR})^2 + [2(1+8Br')/Pe]^2 + Br'(1+\psi\theta_1)(\frac{d\hat{u}}{dR})^2/\psi} \\ &= \big[(16Br'+1)^2R^6 - 4(16Br'+1)(8Br'+1)R^4 \\ &\quad + 4(8Br'+1)^2R^2 + 16(8Br'+1)^2/Pe^2\big] \\ &\quad \big/\big\{(16Br'+1)(8Br'+1)R^6 - 4(8Br'+1)^2R^4 \\ &\quad + 4\big[32Br'^2 + 2(5+8/\psi)Br' + 1\big]R^2 \\ &\quad + 16(8Br'+1)^2/Pe^2\big\} \end{aligned} \tag{22}$$

$Be = 1$ is the limit at which the irreversibility due to heat transfer dominates while $Be = 0$ is the opposite limit where the irreversibility is solely attributed to fluid friction. For the case when the viscous dissipation term is absent in the energy equation, by following the procedures applied in Model 1, the dimensionless entropy generation, its two components and Bejan number for Model 2 are derived, respectively, as

$$\begin{aligned} N_{\text{S2}} &= \left(\frac{\psi}{1+\psi\theta_2}\right)^2\left[\left(\frac{d\theta_2}{dR}\right)^2 + \frac{4}{Pe^2}\right] \\ &\quad + Br'\left(\frac{\psi}{1+\psi\theta_2}\right)\left(\frac{d\hat{u}}{dR}\right)^2 \\ &= 16\big\{(1-8Br')R^6 + 4(8Br'+1)R^4 \\ &\quad + 4\big[2Br'(8/\psi-3)+1\big]R^2 + 16/Pe^2\big\} \\ &\quad /(R^4 - 4R^2 - 8/\psi + 3)^2 \end{aligned} \tag{23}$$

$$\begin{aligned} N_{\text{HT2}} &= \left(\frac{\psi}{1+\psi\theta_2}\right)^2\left[\left(\frac{d\theta_2}{dR}\right)^2 + \frac{4}{Pe^2}\right] \\ &= 16[R^6 - 4R^4 + 4R^2 + 16/Pe^2] \\ &\quad /(R^4 - 4R^2 - 8/\psi + 3)^2 \end{aligned} \tag{24}$$

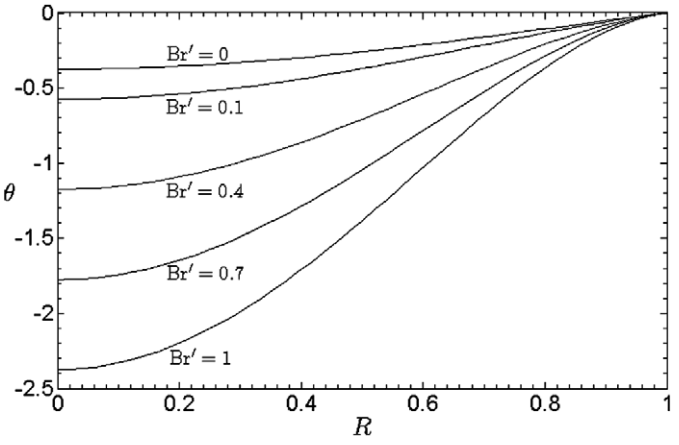

Fig. 1. Dimensionless temperature distribution as a function of radial direction for different Brinkman number.

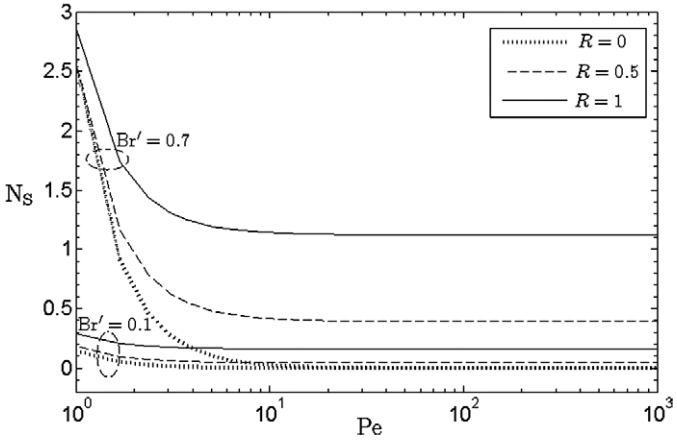

Fig. 2. Dimensionless entropy generation as a function of Péclet number at different radial distances.

$$N_{FF2} = Br'\left(\frac{\psi}{1+\psi\theta_2}\right)\left(\frac{d\hat{u}}{dR}\right)^2 = -128Br'R^2/(R^4 - 4R^2 - 8/\psi + 3) \tag{25}$$

$$Be_2 = \frac{(d\theta_2/dR)^2 + (2/Pe)^2}{(d\theta_2/dR)^2 + (2/Pe)^2 + Br'(1+\psi\theta_2)(d\hat{u}/dR)^2/\psi} = (R^6 - 4R^4 + 4R^2 + 16/Pe^2)/\{(1-8Br')R^6 - 4(1-8Br')R^4 + 4[2Br'(8/\psi - 3) + 1]R^2 + 16/Pe^2\} \tag{26}$$

The average dimensionless entropy generation and average Bejan number, over the circular cross section of the microchannel A_c can be, respectively, computed by the following integrations

$$\bar{N}_S = \frac{1}{A_c}\int_{A_c} N_S\, dA_c = 2\int_0^1 N_S R\, dR, \tag{27}$$

$$\overline{Be} = \frac{1}{A_c}\int_{A_c} Be\, dA_c = 2\int_0^1 BeR\, dR \tag{28}$$

In order to compare Model 1 with Model 2, the relative deviation (in percentage) of the pertinent parameters (N_S, Be, $\bar{N}_S$, $\overline{Be}$) between these two models is quantified as

$$\delta = \frac{m_1 - m_2}{m_1} \times 100\%, \qquad m = N_S, Be, \bar{N}_S, \overline{Be} \tag{29}$$

3. Results and discussion

Fig. 1 shows the dimensionless temperature profiles, representing the temperature difference between the working fluid and the wall of the microchannel, for different Brinkman number. With increasing Brinkman number, higher viscous heating generated in proximity to the wall boundary intensifies the difference between the fluid temperature and the wall temperature. The temperature gradient becomes steeper, indicating that heat transported from the wall to the fluid increases for higher Brinkman number. Thus, from the first-law analysis, it is obvious that the viscous dissipation induces significant effect on the fluid temperature field when the Brinkman number is considerably large, corresponding to the heat transfer behaviour in microchannels.

As mentioned in the preceding section, the axial conduction term in the energy equation, which is inversely proportional to Péclet number Pe, is negligible in the current study. This leads to a high value of Péclet number. Without loss of generality, $Pe^{-2} \to 0$ is thus adopted in the subsequent evaluations of the dimensionless entropy generation and Bejan number. This is justifiable from the exhibition of the effect of Péclet number on the dimensionless entropy generation N_S, at different radial distances in Fig. 2. The dimensionless entropy generation decreases with increasing Péclet number until it reaches an asymptotic value. The order of magnitude of Péclet number for typical working fluids in microchannels is generally ranged from 10^3 to 10^4, in which the dimensionless entropy generation can be deemed independent of Péclet number. Therefore, with negligible effect of Péclet number, and according to Eqs. (16), (22), (23) and (26), the Brinkman number Br' and the dimensionless heat flux ψ are the variable parameters in the dimensionless entropy generation and Bejan number functions. Following this, it should be noted that zero value of velocity and temperature gradients at the centerline will lead to singularities in Bejan number (for both models) and the relative deviation δ of the pertinent parameters, defined in Eqs. (22), (26) and (29), respectively.

For the case when viscous dissipation effect is not included in the energy equation, the volumetric rate of entropy generation rate can be expressed in terms of the irreversibility distribution ratio ϕ as

$$\dot{S}'''_{gen}\frac{kT_w^2}{q_w^2} = \frac{(1+\phi)[(2R - R^3)^2 + 16/Pe^2]}{[\psi(-R^4/8 + R^2/2 - 3/8) + 1]^2} \tag{30}$$

For $Pe^{-2} \to 0$ and in the limit of $\psi \to 0$, the dimensionless radial entropy generation profiles as expressed in Eq. (30) are plotted for different ϕ in Fig. 3. In this case, being independent on the applied heat flux at the boundary wall, the dimensionless entropy generation is ascribable to the irreversibility due to radial conductive heat transfer governed by the radial temperature gradient and the irreversibility due to fluid friction governed

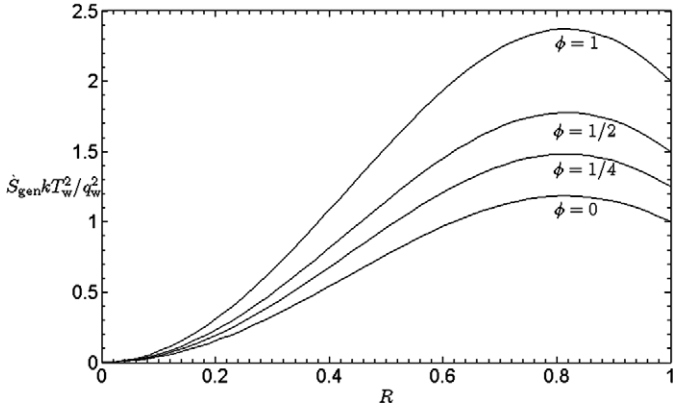

Fig. 3. Radial entropy generation profiles for different irreversibility distribution ratio in the limit of $Pe^{-2} \to 0$ and $\psi \to 0$ when the viscous dissipation effect is not included.

by the radial velocity gradient, as shown in Eq. (30). The dimensionless entropy generation is zero at the centerline region due to zero velocity and temperature gradients in the centre of the channel. The radial velocity gradient varies linearly with the radial distance of the channel, implying that there is no inherent extremum in the fluid friction irreversibility across the cross section, hence it can be observed that the dimensionless entropy generation reaches its maximum at a fixed location at $R = \sqrt{2/3}$ for all values of ϕ corresponding to the occurrence of maximum radial temperature gradient, attributed to the effect of wall curvature [25]. As ϕ increases, the viscous effect becomes prominent and higher fluid friction irreversibility contributes to higher entropy generation across the cross section. For frictionless case with $\phi = 0$, the radial entropy generation profile is identical to the $\dot{S}'''_{gen} kT_0^2/q_w^2$ profile plotted by Bejan [26] under the same hydrodynamic and thermal conditions for a round smooth tube, where T_0 is the absolute temperature at a point of origin located on the tube axis. Under such circumstances, Eq. (30) is reduced to

$$\dot{S}'''_{gen} \frac{kT_w^2}{q_w^2} = (2R - R^3)^2 \tag{31}$$

demonstrating an expression which is identical with that derived in [26]. To this end, as noticed that the dimensionless entropy generation in the present study is dependent on the Brinkman number Br' and the dimensionless heat flux ψ, the analysis of the entropy generation in a microchannel is based on the effect of viscous dissipation, which is characterised by the Brinkman number and the effect imposed by the dimensionless heat flux. Attention is focused on the comparison between the models with and without considering viscous dissipation effect by analyzing their relative deviations in local and average dimensionless entropy generation and Bejan number, which are discussed in the following.

3.1. Effect of viscous dissipation

Figs. 4(a) and 4(b) show the radial dimensionless entropy generation and Bejan number distributions at a fixed value of dimensionless heat flux ($\psi = 0.1$) for $Br' = 0.1$ and $Br' = 0.7$, respectively. The relative deviations of dimensionless entropy generation and Bejan number between Model 1 and Model 2, as defined in Eq. (29), are also depicted in the figures. Entropy generation increases tremendously from zero at the centre of the channel to a maximum value at the wall. This is due to the velocity and temperature gradients are zero at the centerline in stark contrast to the comparatively high values in the vicinity of the wall. Comparing Figs. 4(a) and 4(b), it is observed that the dimensionless entropy generation (for both models) increases with increasing Brinkman number. On the contrary, Bejan number shows the opposite trend, in which it is minimum at the wall and peaks at the centre of the channel. This indicates that the maximum entropy produced at the wall is mainly due to the fluid friction irreversibility and compensated by the heat transfer irreversibility towards the centre of the channel with zero entropy generation. It is known that $\dot{S}'''_{HT}$ will only surpass $\dot{S}'''_{FF}$ if $Be > 0.5$. Hence one can deduce that most of the entropy generated in the microchannel (for both models) is attributed to the fluid friction irreversibility when the dimensionless heat flux ψ is small. If one compares the Bejan number distributions for Model 1 and Model 2, it is observed that for Model 1, Bejan number increases with higher Brinkman number whereas for Model 2, Bejan number decreases as Brinkman number increases. This indicates that with increasing Brinkman number, the dominance of fluid friction irreversibility decreases and the contribution of heat transfer irreversibility increases when the viscous dissipation is taken into account in the energy equation. This phenomenon can be further explained by Figs. 5(a) and 5(b), which show the distributions of dimensionless entropy generation by heat transfer contribution N_{HT} and dimensionless fluid friction contribution N_{FF} (for Model 1 and Model 2) at $\psi = 0.1$ for different Brinkman number, respectively. N_{FF} displays zero value at the centerline and reaches a maximum value at the wall of the channel. The high value of N_{FF} adjacent to the wall is contributed by the high near wall velocity gradient. For the case of small dimensionless heat flux, it is noted that when Brinkman number is small ($Br' = 0.1$), N_{FF1} and N_{FF2} are almost overlapping, showing that the viscous dissipation effect on the fluid friction irreversibility is negligible, while for higher Brinkman number ($Br' = 0.7$), the viscous dissipation effect induced on the fluid friction irreversibility is also not obvious in this case. Comparing Fig. 5(a) and Fig. 5(b), it is observed that the magnitude of N_{HT} is relatively small compared to N_{FF}, indicating that the contribution of the heat transfer irreversibility to the total entropy generation is negligible in this case. However, comparing Model 1 and Model 2, $N_{HT1}$is significantly higher than N_{HT2}. This is because the heat transfer irreversibility is strongly dependent on the temperature field, as expressed in Eqs. (19) and (24). Neglecting viscous dissipation effect in the first-law analysis will indirectly incur significant deviation on the heat transfer irreversibility.

Examining the relative deviations of dimensionless entropy generation and Bejan number between Model 1 and Model 2 in Figs. 4(a) and 4(b), one can observe that the relative deviation of N_S is relatively insignificant (less than 10%) at small Brinkman number ($Br' = 0.1$), whereas for larger Brinkman number ($Br' = 0.7$), the relative deviation increases and amounts to a

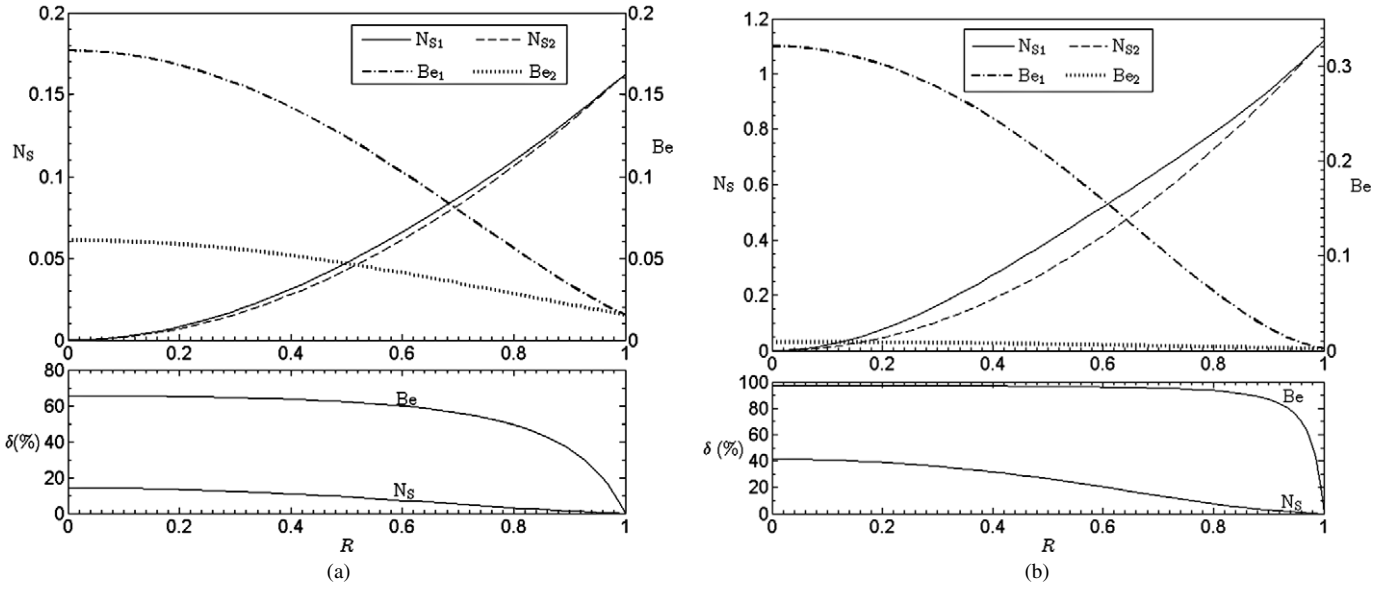

Fig. 4. Dimensionless entropy generation and Bejan number distributions in the radial direction at $\psi = 0.1$ for (a) $Br' = 0.1$, (b) $Br' = 0.7$.

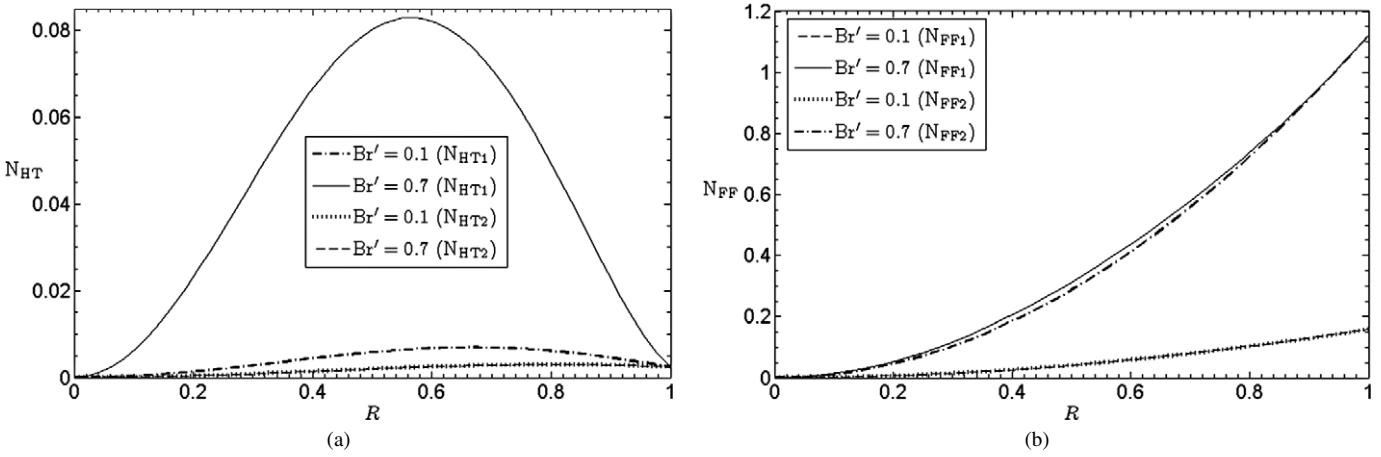

Fig. 5. Dimensionless entropy generation due to (a) heat transfer irreversibility, and (b) fluid friction irreversibility, at $\psi = 0.1$ for different Brinkman number.

maximum of about 40% adjacent to the centerline. This indicates that the relative deviation of N_S increases with increasing Brinkman number. For Bejan number, the relative deviation between Model 1 and Model 2 is prominent (more than 60% and 90% over the cross section for $Br' = 0.1$ and $Br' = 0.7$, respectively, except in the vicinity to the wall) indicating that viscous dissipation significantly affect the Bejan number profile. This is attributed to the strong dependence of heat transfer irreversibility on the fluid temperature distribution, as explained in the preceding paragraph.

3.2. Effect of dimensionless heat flux

The dimensionless entropy generation and Bejan number increase in value, when the dimensionless heat flux rises to $\psi = 0.4$, as illustrated in Figs. 6(a) and 6(b). In this case, the contribution of the heat transfer irreversibility becomes manifest and the entropy generation is no more governed by the fluid friction irreversibility, as shown in Figs. 7(a) and 7(b). Simultaneously, with increasing dimensionless heat flux, the loss contributed by fluid friction irreversibility (for both models) also increases and the difference of fluid friction irreversibility between Model 1 and Model 2 is also enlarged. Due to the increasing importance of heat transfer irreversibility, and correspondingly the increase in the difference of fluid friction irreversibility, the relative deviation on the entropy generation becomes much higher, compared to the case of lower dimensionless heat flux. This is manifested in Figs. 6(a) and 6(b), where there are dramatic rises in the relative deviations of dimensionless entropy generation to more than 40% and 90% adjacent to the centerline for $Br' = 0.1$ and $Br' = 0.7$, respectively. In the case of higher dimensionless heat flux, viscous dissipation induces significant effect on the temperature field, which in turn affects the heat transfer irreversibility and fluid friction irreversibility in a more extensive manner. Hence, higher relative deviation on the entropy generation is observed when the dimensionless heat flux increases.

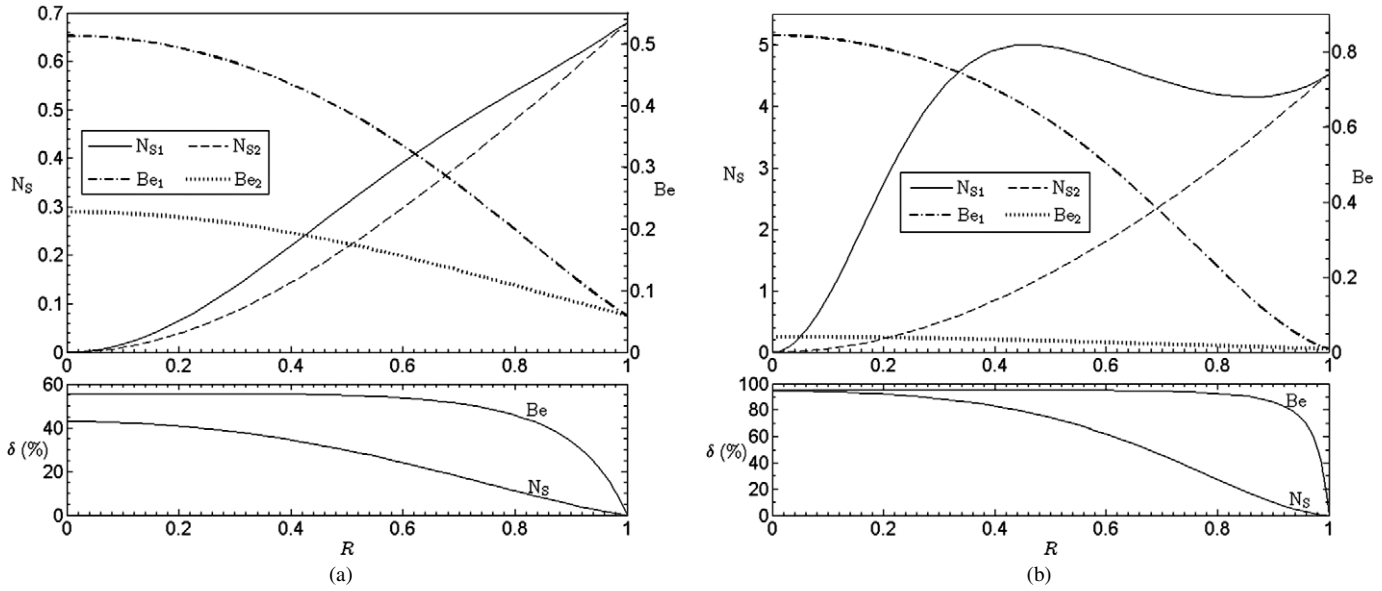

Fig. 6. Dimensionless entropy generation and Bejan number distributions in the radial direction at $\psi = 0.4$ for (a) $Br' = 0.1$, (b) $Br' = 0.7$.

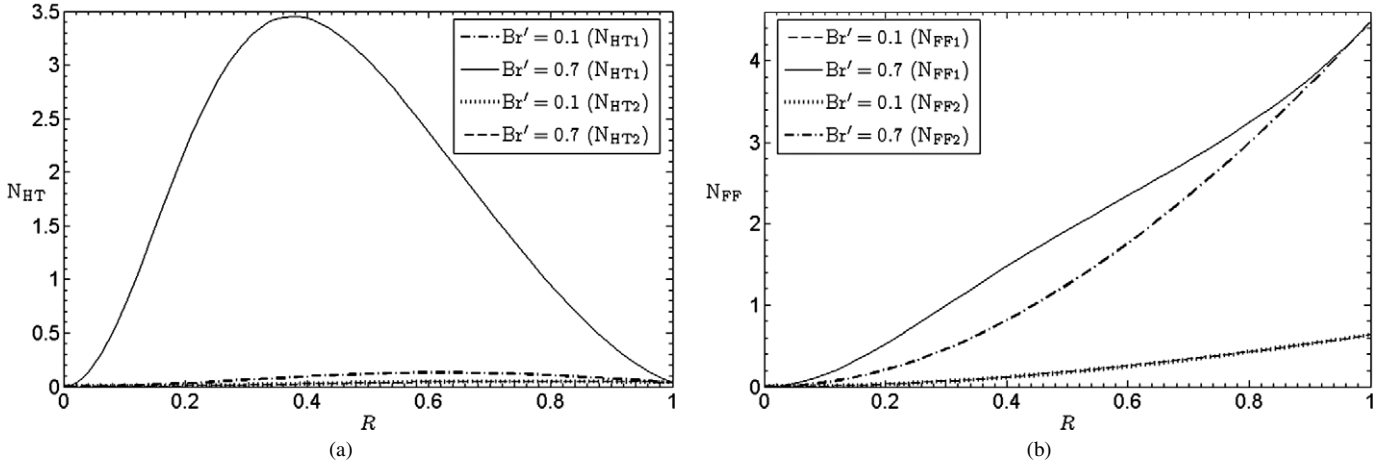

Fig. 7. Dimensionless entropy generation due to (a) heat transfer irreversibility, and (b) fluid friction irreversibility, at $\psi = 0.4$ for different Brinkman number.

3.3. Average dimensionless entropy generation and Bejan number

Fig. 8 plots average dimensionless entropy generation $\bar{N}_S$ and average Bejan number $\overline{Be}$ as a function of Brinkman number for fixed value of dimensionless heat flux ($\psi = 0.1$). The relative deviations of average dimensionless entropy generation and average Bejan number between Model 1 and Model 2, as a function of Brinkman number, are also shown in the figure. It is observed that the average dimensionless entropy generation (for both models) increases with increasing Brinkman number. Average Bejan number (for both models) exhibits high value when Brinkman number is very close to zero and decreases to a minimum value, after which the average Bejan number for Model 1 increases with small gradient with increasing Brinkman number whereas for Model 2, the average Bejan number slightly decreases as Brinkman number increases. For both models, except for small Brinkman number, the distribution of average Bejan number matches the observation for local Bejan number, as explained earlier in Section 3.1. As expected, the relative deviations of average dimensionless entropy generation and average Bejan number increase with increasing Brinkman number, attributable to the increasing effect of viscous dissipation on the heat transfer irreversibility, as explained earlier.

Fig. 9 illustrates the variations of average dimensionless entropy generation $\bar{N}_S$ and average Bejan number $\overline{Be}$ as well as their relative deviations between Model 1 and Model 2, as a function of dimensionless heat flux for fixed value of Brinkman number ($Br' = 0.1$). In the preceding discussion, it is known that the contribution of heat transfer irreversibility and fluid friction irreversibility increases with increasing dimensionless heat flux. Hence, it is conceivable that the average dimensionless entropy generation and average Bejan number (for both models) increase with increasing dimensionless heat flux. This also leads to a larger relative deviation of the average dimensionless entropy generation when the dimensionless heat flux increases, indicating that the viscous dissipation effect on the entropy generation is more significant for higher dimensionless

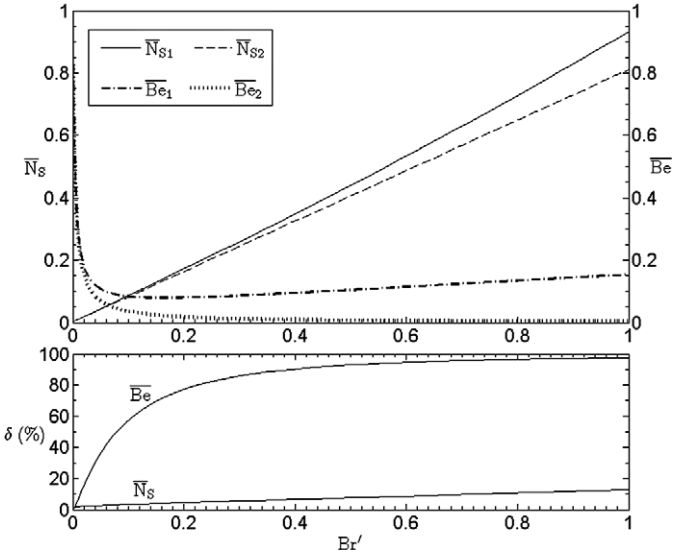

Fig. 8. Average dimensionless entropy generation and Bejan number distributions as a function of Br' at $\psi = 0.1$.

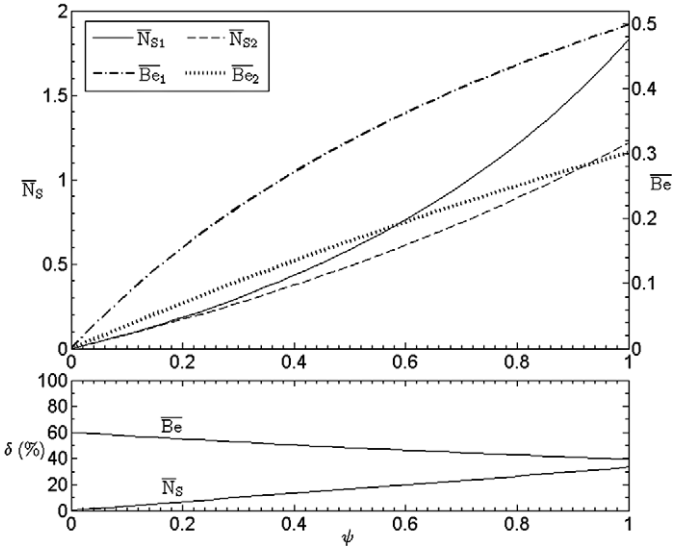

Fig. 9. Average dimensionless entropy generation and Bejan number distributions as a function of ψ at $Br' = 0.1$.

heat flux. On the other hand, the gradual decline in the relative deviation of average Bejan number is due to the scaling effect of the increasing value of the denominator in Eq. (29), in which case the average Bejan number for Model 1 increases faster than the difference with its counterpart for Model 2.

4. Conclusions

A mathematical model based on the first law and second law of thermodynamics of circular microchannels during steady-state operation has been developed, to investigate, primarily, the effect of the viscous dissipation on the entropy generation assessments and a better understanding of the physical problem is reached. This investigation provides interesting insights into the phenomena which take place in the comparison between the models with and without viscous dissipation effect on the assessments of entropy generation in microchannels. The analysis of entropy generation by examining the influence of the pertinent parameters in this study would be a useful analytical tool for engineering design and performance evaluation of such heat exchange devices based on the second law of thermodynamics which are essential for more effective use of available energy by reducing the destruction of useful potential work. It is found that in this study when the viscous dissipation is taken into account, the temperature distribution is a strong function of the Brinkman number. Consequently, the entropy generation, ascribable to the heat transfer irreversibility and fluid friction irreversibility, is also intimately related to the Brinkman number under the influence of viscous dissipation. It is evident that the relative deviation of dimensionless entropy generation and Bejan number between the models with and without considering the viscous dissipation effect increases as Brinkman number and dimensionless heat flux increase. The variations of the relative deviations result from the effect induced by viscous dissipation on the heat transfer irreversibility and fluid friction irreversibility, which are the two major components of entropy generation in channel flow. It can be concluded that the influence of viscous dissipation on the entropy generation is significant albeit not dominant especially for the cases of high Brinkman number and dimensionless heat flux.

References

[1] A. Bejan, Entropy Generation Minimization, CRC Press, Boca Raton, 1995.
[2] R.K. Shah, D.P. Sekulić, Fundamentals of Heat Exchanger Design, Wiley, New York, 2003, pp. 796–801.
[3] C.P. Tso, S.P. Mahulikar, The use of the Brinkman number for single phase forced convective heat transfer in microchannels, Int. J. Heat Mass Transfer 41 (1998) 1759–1769.
[4] C.P. Tso, S.P. Mahulikar, Experimental verification of the role of Brinkman number in microchannels using local parameters, Int. J. Heat Mass Transfer 43 (2000) 1837–1849.
[5] J. Judy, D. Maynes, B.W. Webb, Characterization of frictional pressure drop for liquid flows through microchannels, Int. J. Heat Mass Transfer 45 (2002) 3477–3489.
[6] J. Koo, C. Kleinstreuer, Viscous dissipation effects in microtubes and microchannels, Int. J. Heat Mass Transfer 47 (2004) 3159–3169.
[7] G.L. Morini, Viscous heating in liquid flows in micro-channels, Int. J. Heat Mass Transfer 48 (2005) 3637–3647.
[8] G. Hetsroni, A. Mosyak, E. Pogrebnyak, L.P. Yarin, Heat transfer in microchannels: comparison of experiments with theory and numerical results, Int. J. Heat Mass Transfer 48 (2005) 5580–5601.
[9] D.P. Sekulić, A. Campo, J.C. Morales, Irreversibility phenomena associated with heat transfer and fluid friction in laminar flows through singly connected ducts, Int. J. Heat Mass Transfer 40 (1997) 905–914.
[10] Y. Demirel, H.H. Al-Ali, Thermodynamic analysis of convective heat transfer in a packed duct with asymmetrical wall temperatures, Int. J. Heat Mass Transfer 40 (1997) 1145–1153.
[11] A.Z. Şahin, Second law analysis of laminar viscous flow through a duct subjected to constant wall temperature, J. Heat Transfer 120 (1998) 76–83.
[12] A.Z. Şahin, Irreversibilities in various duct geometries with constant wall heat flux and laminar flow, Energy 23 (1998) 465–473.
[13] A.Z. Şahin, The effect of variable viscosity on the entropy generation and pumping power in a laminar fluid flow through a duct subjected to constant heat flux, Heat Mass Transfer 35 (1999) 499–506.
[14] Y. Demirel, R. Kahraman, Thermodynamic analysis of convective heat transfer in an annular packed bed, Int. J. Heat Fluid Flow 21 (2000) 442–448.

[15] S. Mahmud, R.A. Fraser, The second law analysis in fundamental convective heat transfer problems, Int. J. Thermal Sci. 42 (2003) 177–186.
[16] S. Mahmud, R.A. Fraser, Analysis of entropy generation inside concentric cylindrical annuli with relative rotation, Int. J. Thermal Sci. 42 (2003) 513–521.
[17] E.B. Ratts, A.G. Raut, Entropy generation minimization of fully developed internal flow with constant heat flux, J. Heat Transfer 126 (2004) 656–659.
[18] D.H. Richardson, D.P. Sekulić, A. Campo, Low Reynolds number flow inside straight micro channels with irregular cross sections, Heat Mass Transfer 36 (2000) 187–193.
[19] L.B. Erbay, M.M. Yalçin, M.Ş. Ercan, Entropy generation in parallel plate microchannels, Heat Mass Transfer 43 (2007) 729–739.
[20] H. Abbassi, Entropy generation analysis in a uniformly heated microchannel heat sink, Energy 32 (2007) 1932–1947.
[21] M. Gad-el-Hak, The fluid mechanics of microdevices – the Freeman scholar lecture, J. Fluids Eng. 121 (1999) 5–33.
[22] A. Bejan, Convection Heat Transfer, third ed., Wiley, New York, 2004, pp. 1–119.
[23] B.-X. Wang, X.F. Peng, Experimental investigation on liquid forced-convection heat transfer through microchannels, Int. J. Heat Mass Transfer 37 (1994) 73–82.
[24] W. Kays, M. Crawford, B. Weigand, Convective Heat and Mass Transfer, fourth ed., McGraw Hill, New York, 2005, pp. 91–92.
[25] A. Bejan, A study of entropy generation in fundamental convective heat transfer, J. Heat Transfer 101 (1979) 718–725.
[26] A. Bejan, Entropy Generation Through Heat and Fluid Flow, Wiley-Interscience, New York, 1982, pp. 98–105.